

Supplementary Information for “Towards a formation model of the Neanderthal symbolic accumulation of herbivore crania in the Lozoya Valley: Spatial Patterns Shaped by Rockfall Dynamics in Level 3 of Des-Cubierta Cave”

Journal name: Archaeological and Anthropological Sciences

Authors: Lucía Villaescusa^{1,2 *}, Enrique Baquedano^{2,3}, David M. Martín-Perea⁴, Belén Márquez², M. Ángeles Galindo-Pellicena^{1,2}, Lucía Cobo-Sánchez⁵, Ana Isabel Ortega⁶, Rosa Huguet^{7,8,9}, César Laplana^{10,2}, M. Cruz Ortega¹¹, Sandra Gómez-Soler^{12,13,2}, Abel Moclán^{14,3}, Nuria García^{4,11}, Diego J. Álvarez-Lao¹⁵, Rebeca García-González¹⁶, Laura Rodríguez^{16,17}, Alfredo Pérez-González³, Juan Luis Arsuaga^{4,11}

¹ Departament of Geology, Geography and Environment Science, Universidad de Alcalá de Henares, Alcalá de Henares, España

² Museo Arqueológico y Paleontológico de la Comunidad de Madrid, Alcalá de Henares, España

³ Institute of Evolution in Africa – IDEA, Madrid, Spain

⁴ Department of Geodynamics, Stratigraphy and Palaeontology, Faculty of Geology, Complutense University of Madrid, Madrid, Spain

⁵ Interdisciplinary Center for Archaeology and the Evolution of Human Behaviour (ICArEHB), Universidade do Algarve, Campus de Gambelas, 8005-139 Faro, Portugal

⁶ Independent researcher, Burgos, Spain

⁷ IPHES-CERCA, Institut Català de Paleoecologia Humana i Evolució Social, Tarragona, España

⁸ Departament d'Història i Història de l'Art, University Rovira i Virgili, Tarragona, España

⁹ Unit associated to CSIC, Departamento de Paleobiología, Museo Nacional de Ciencias Naturales, Madrid, Spain

¹⁰ Grupo UAH Arqueo-Paleontología de la Evolución Humana, Universidad de Alcalá, España

¹¹ UCM-ISCIH Research Center of Human Evolution and Behavior, Madrid, Spain

¹² Archaeological Micromorphology and Biomarkers Laboratory (AMBi Lab), Instituto Universitario de Bio-orgánica “Antonio González”, La Laguna University, Tenerife, Spain

¹³ Department of History and Philosophy, University of Alcalá de Henares, Madrid, Spain

¹⁴ PALEVOPRIM Lab, UMR 7262, CNRS and Université de Poitiers, Poitiers, France

¹⁵ (DA-L) Geology Department, Oviedo University, Oviedo, Spain

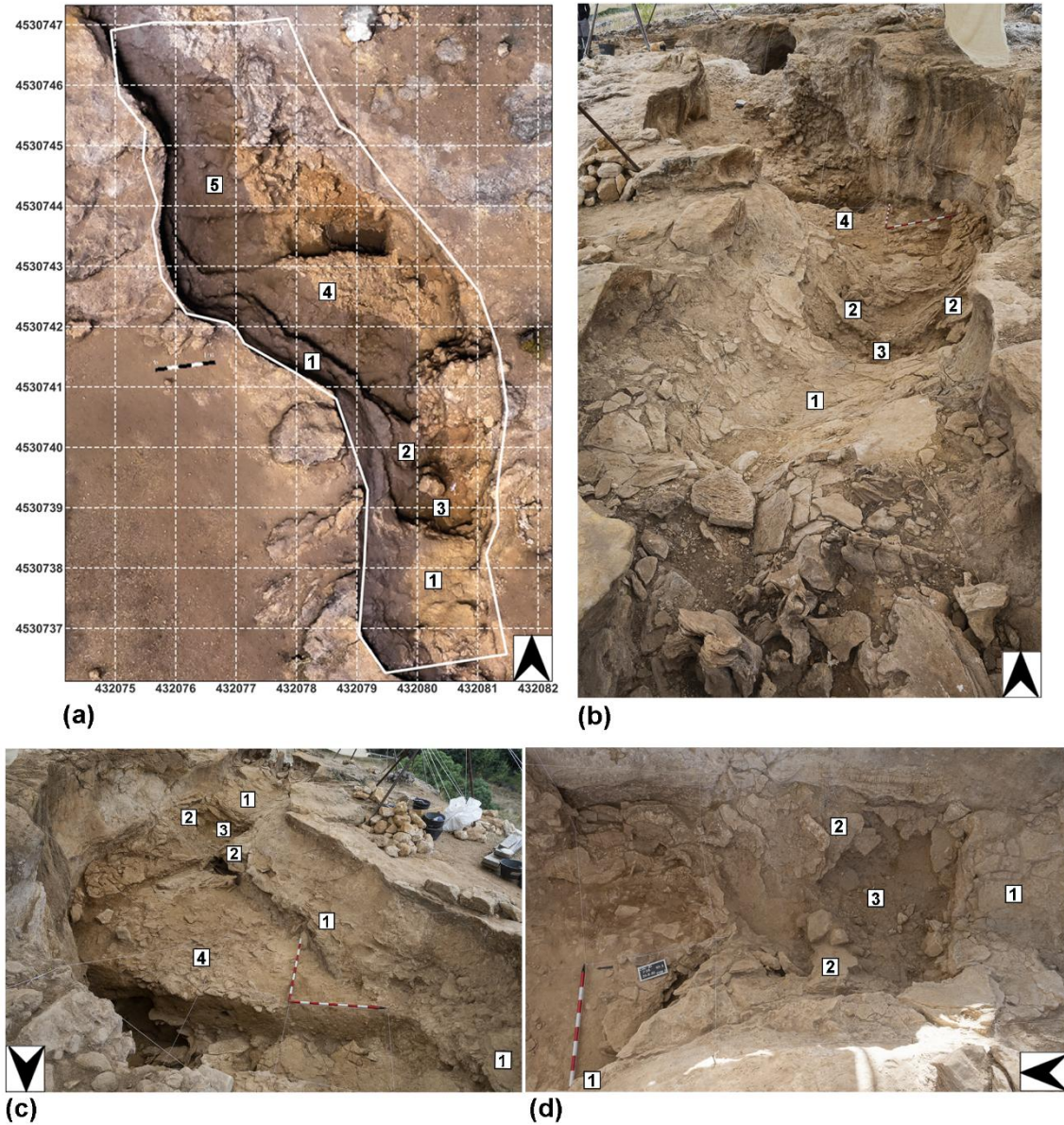
¹⁶ Laboratorio de Evolución Humana, Facultad de Humanidades y Comunicación, Universidad de Burgos, España

¹⁷ Área de Antropología Física. Facultad de Cc. Biológicas y Ambientales. Universidad de León, España

*Corresponding author mail: lucia.villaescusa.fernandez@gmail.com

Supplementary Information 1

Figures: (a) Photogrammetric model of the Des-Cubierta Cave gallery where Level 3 was deposited; (b) view from the south of the same gallery area; (c) view from the north; (d) top view of the narrowing zone. **Numbered elements:** (1) S1 speleotheme *in situ*; (2) imbricated and verticalized S1 speleotheme fragments; (3) cuvette-shaped depression in the narrowing zone; (4) Unit 4 prismatic blocks; (5) top of Unit 5



Supplementary Information 2. Table summarizing the method selected to estimate the sigma parameter for the kernel density analyses, including any applied adjustments and the final calculated value

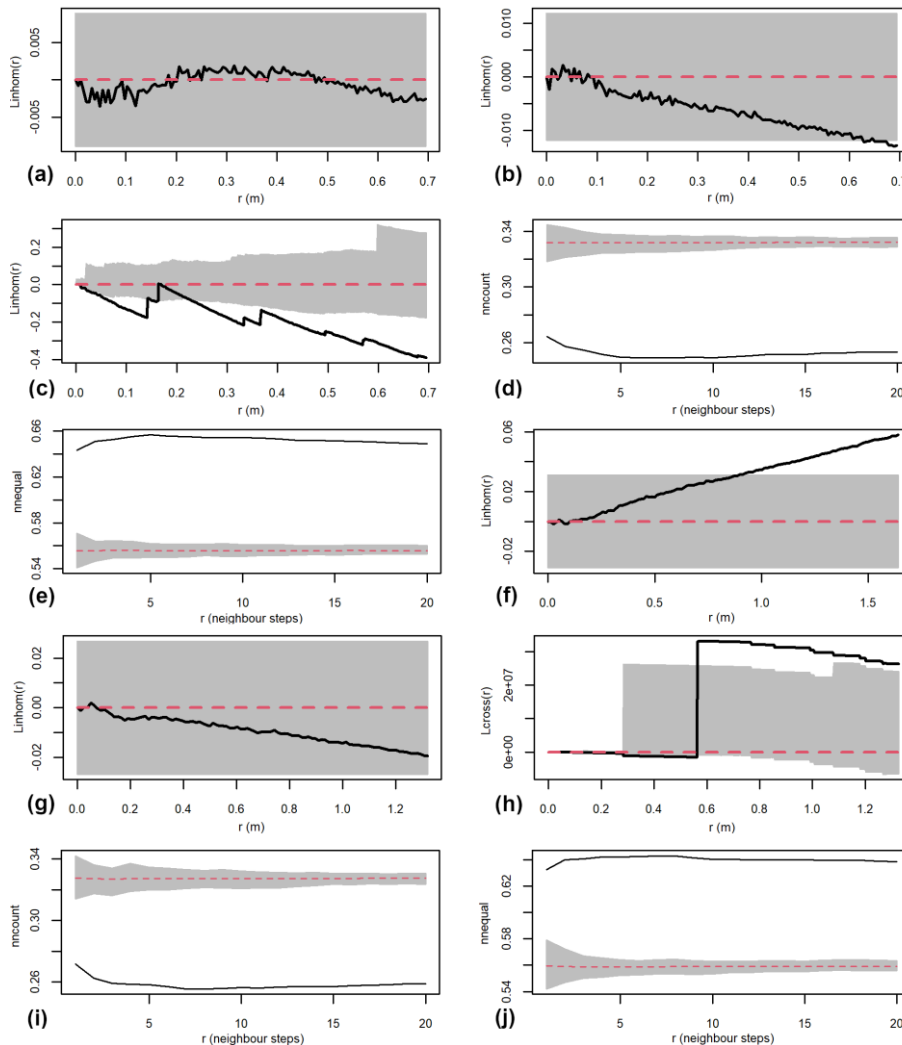
Material	View	Sigma method and adjust	Sigma value
Archaeological	Plan	bw.ppl*2	0.084
	Section	bw.ppl*2	0.136
Clasts	Plan	bw.ppl	0.283
	Section	bw.ppl	0.205
Large boulder	Plan	bw.ppl	0.635
	Section	bw.ppl*0.5	0.257
Medium boulder	Plan	bw.ppl	0.306
	Section	bw.ppl	0.193
Small boulder	Plan	bw.ppl*0.5	0.153
	Section	bw.ppl*0.5	0.096
Medium boulder (1st fall)	Plan	bw.ppl*0.5	0.153
Small boulder (1st fall)	Plan	bw.ppl*0.5	0.10

Supplementary information 3

Section analyses: The inhomogeneous L function was applied to the geological (a) and archaeological (b) spatial patterns. While both patterns exhibit distinct trends, neither shows statistically significant deviations overall. The geological pattern tends toward randomness, whereas the archaeological pattern displays a regularity trend (negative values), becoming significant after 65 cm. The Lcross function applied to the marked pattern of geological and archaeological materials (c) indicates a negative correlation between the two material types. The results of the neighborhood-based functions reinforce this pattern, with the nncount function (d) showing a highly significant segregation between geological and archaeological materials, while the nnequal function (e) highlights their strong within-type aggregation.

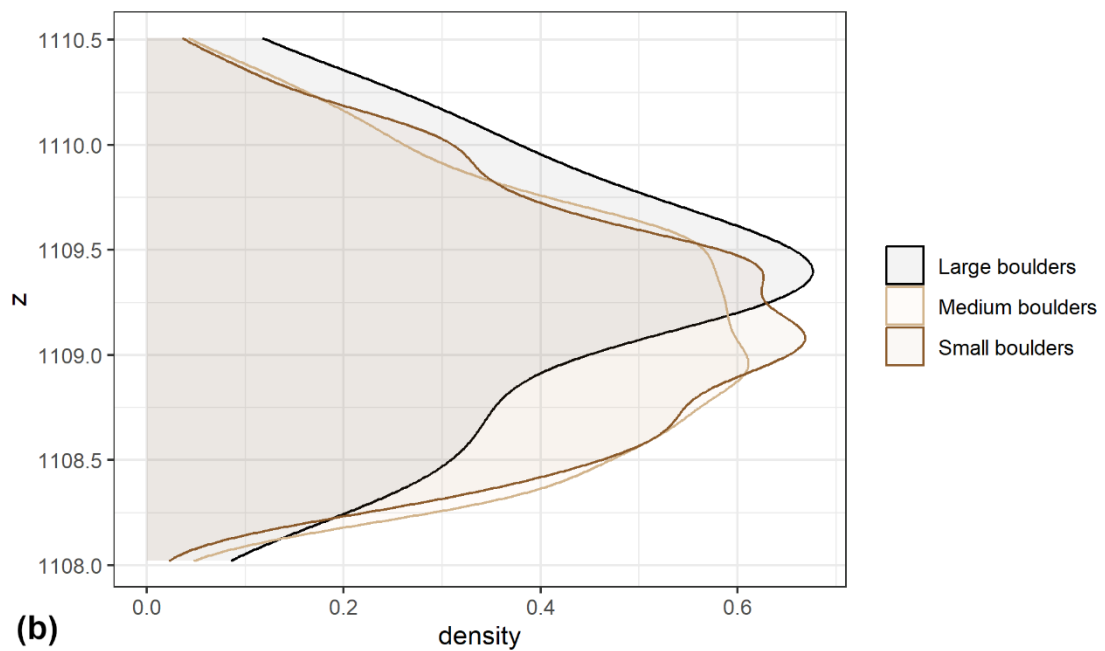
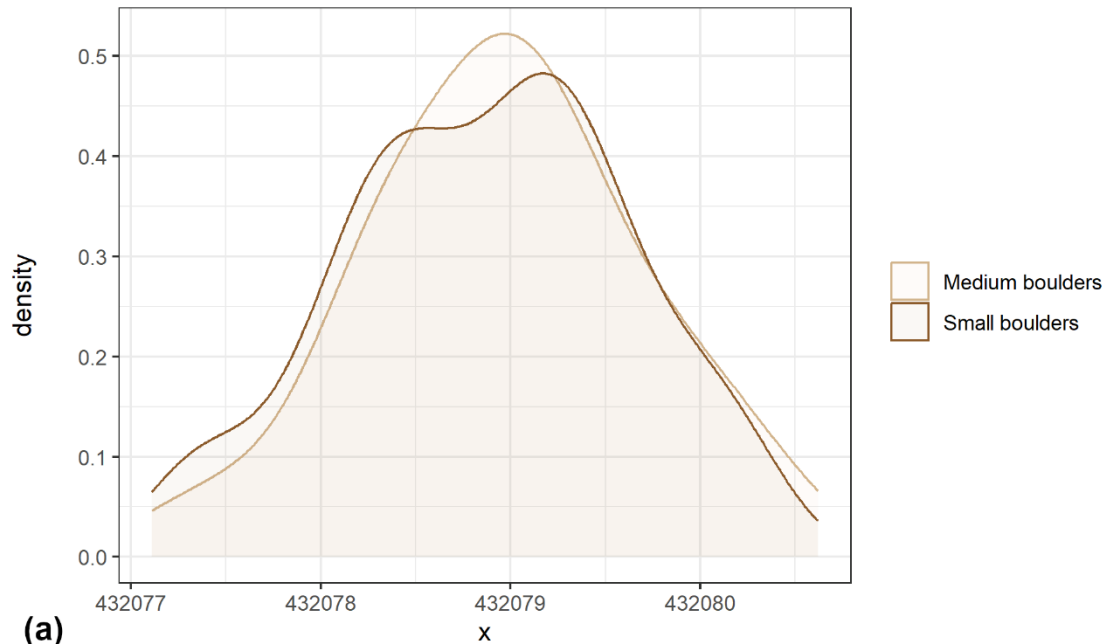
Plan analyses: The inhomogeneous L function applied to the geological (f) and archaeological (g) spatial patterns reveals different behaviors. The geological pattern exhibits an aggregation tendency after 1 meter, whereas the archaeological pattern follows a random distribution. The Lcross function (h) shows a negative correlation between material types, which shifts sharply to a positive correlation after 0.55 meters. This sudden change suggests that the function may not be adequately capturing the pattern's structure. Better results were obtained with nncount (i) and nnequal (j), confirming a highly significant segregation of geological and archaeological materials and a strong within-type aggregation.

For the Linhom and Lcross function graphs (a, b, c, f, g, h), values are centered around 0 to enhance the interpretation of deviations from the null hypothesis.

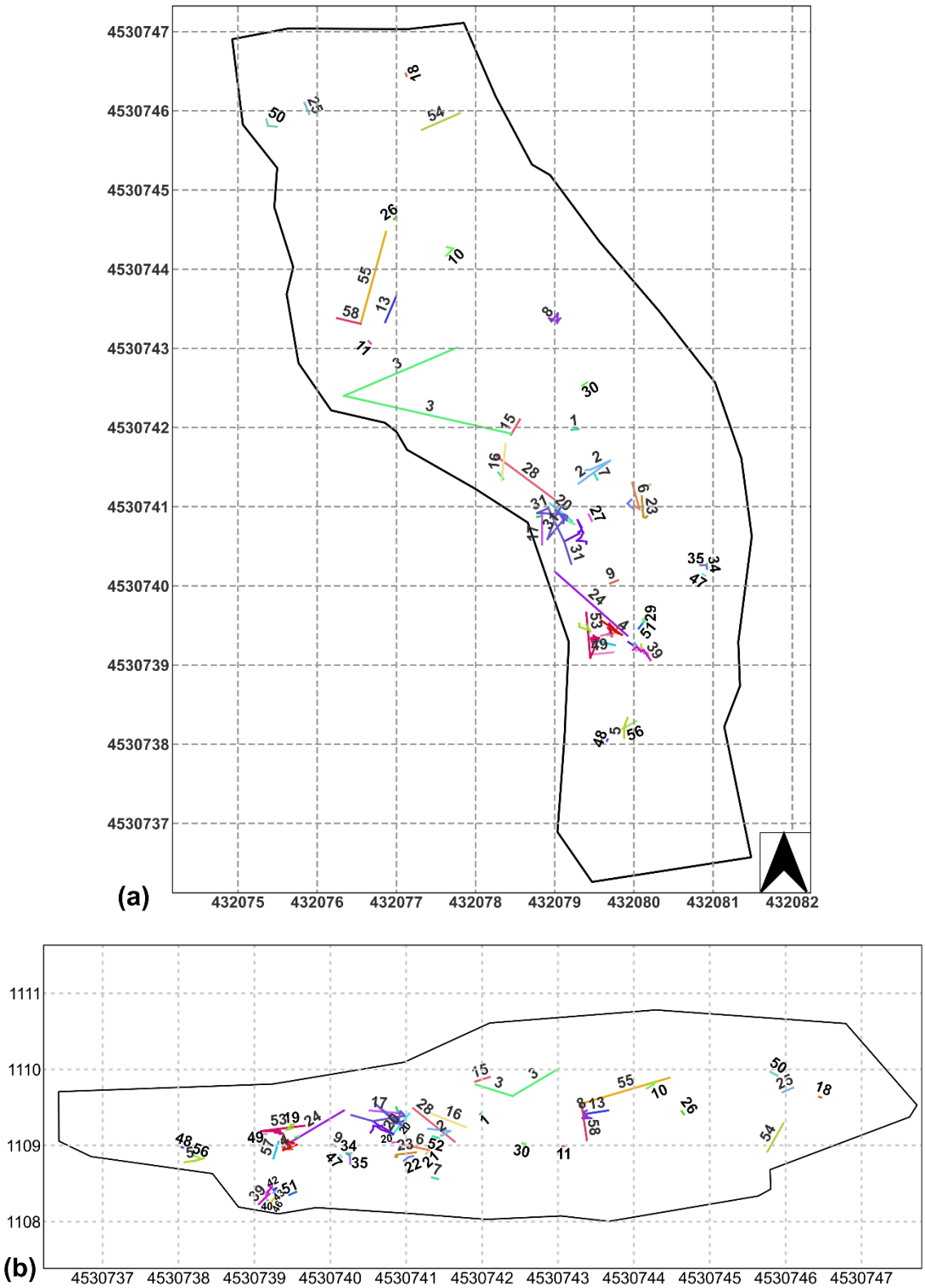


Supplementary Information 4

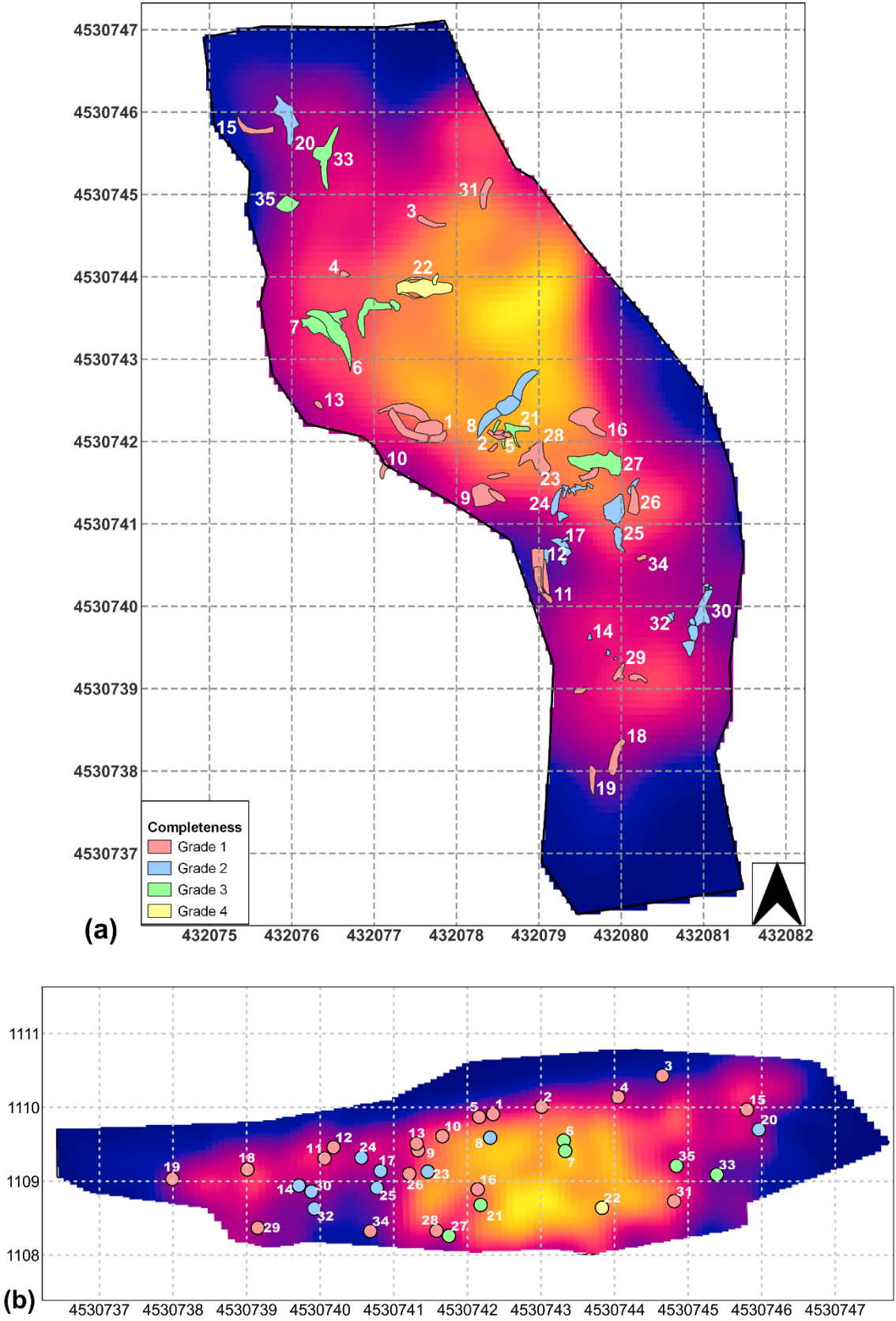
Density of boulders by size: horizontal distribution (x-axis) of boulders located in the area devoid of archaeological materials at the base of Level 3 **(a)**, and vertical distribution (z-axis) of all boulders from Level 3 **(b)**. Both graphs show some extent of sorting by size, as evidenced by the contrasting peaks for each size.



Supplementary Information 5. Detail of refitting line pattern from Level 3 with the numbers of the refits in plan view (a) and section view (b).



Supplementary Information 6. Detail of numbered crania categorized by grades of completeness, overlaid on the medium boulder KDE map in plan view (a) and section view (b).



Supplementary Information 7. Details of the rhinoceros crania and their association with the cone's apex and the first rockfall episode. (a) Plan view and (b) section view showing the distribution of rhinoceros crania by completeness grade, overlaid on the medium boulder KDE map and the clasts from the first rockfall episode. (c) Cranium 22 during fieldwork, illustrating its exceptional preservation. (d) Cranium 27, in a inverted position, during excavation

